

Marquette University

e-Publications@Marquette

Chemistry Faculty Research and Publications

Chemistry, Department of

7-1-2014

Electrochemistry and Spectroelectrochemistry of 1,4-Dinitrobenzene in Acetonitrile and Room-Temperature Ionic Liquids: Ion-Pairing Effects in Mixed Solvents

Abderrahman Atifi
Marquette University

Michael D. Ryan
Marquette University, michael.ryan@marquette.edu

Follow this and additional works at: https://epublications.marquette.edu/chem_fac

 Part of the [Chemistry Commons](#)

Recommended Citation

Atifi, Abderrahman and Ryan, Michael D., "Electrochemistry and Spectroelectrochemistry of 1,4-Dinitrobenzene in Acetonitrile and Room-Temperature Ionic Liquids: Ion-Pairing Effects in Mixed Solvents" (2014). *Chemistry Faculty Research and Publications*. 479.
https://epublications.marquette.edu/chem_fac/479

Electrochemistry and Spectroelectrochemistry of 1,4-Dinitrobenzene in Acetonitrile and Room-Temperature Ionic Liquids: Ion-Pairing Effects in Mixed Solvents

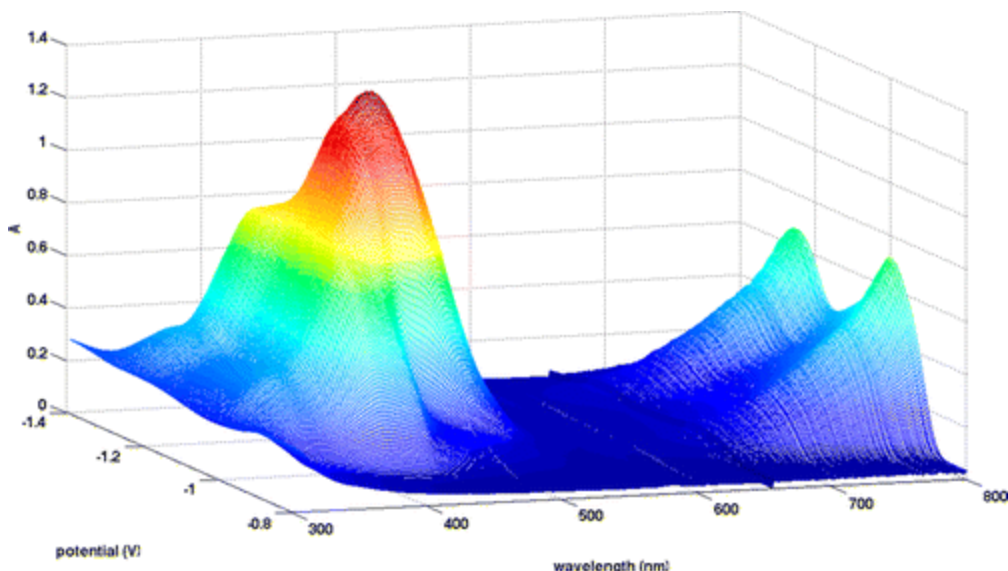
Abderrahman Atifi

*Chemistry Department, Marquette University,
Milwaukee, WI*

Michael D. Ryan

*Chemistry Department, Marquette University,
Milwaukee, WI*

Abstract



Room-temperature ionic liquids (RTILs) have been shown to have a significant effect on the redox potentials of compounds such as 1,4-dinitrobenzene (DNB), which can be reduced in two one-electron steps. The most noticeable effect is that the two one-electron waves in acetonitrile collapsed to a single two-electron wave in a RTIL such as butylmethyl imidazolium- BF_4 (BMIm BF_4). In order to probe this effect over a wider range of mixed-molecular-solvent/RTIL solutions, the reduction process was studied using UV-vis spectroelectrochemistry. With the use of spectroelectrochemistry, it was possible to calculate readily the difference in E° 's between the first and second electron transfer ($\Delta E_{12}^\circ = E_1^\circ - E_2^\circ$) even when the two one-electron waves collapsed into a single two-electron wave. The spectra of the radical anion and dianion in BMIm PF_6 were obtained using evolving factor analysis (EFA). Using these spectra, the concentrations of DNB, DNB $^{\cdot-}$, and DNB $^{2-}$ were calculated, and from these concentrations, the ΔE_{12}° values were calculated. Significant differences were observed when the bis(trifluoromethylsulfonyl)imide (NTf $_2$) anion replaced the PF_6^- anion, leading to an irreversible reduction of DNB in BMImNTf $_2$. The results were consistent with the protonation of DNB $^{2-}$, most likely by an ion pair between DNB $^{2-}$ and BMIm $^+$, which has been proposed by Minami and Fry. The differences in reactivity between the PF_6^- and NTf $_2^-$ ionic liquids were interpreted in terms of the tight versus loose ion pairing in RTILs. The results indicated that nanostructural domains of RTILs were present in a mixed-solvent system.

Multielectron reductions of organic compounds typically occur in sequential one-electron steps. The difference in the E° values (ΔE_{12}°) between the first (E_1°) and second (E_2°) is generally over 200 mV, where $\Delta E_{12}^\circ = E_1^\circ - E_2^\circ$. For example, two one-electron waves were

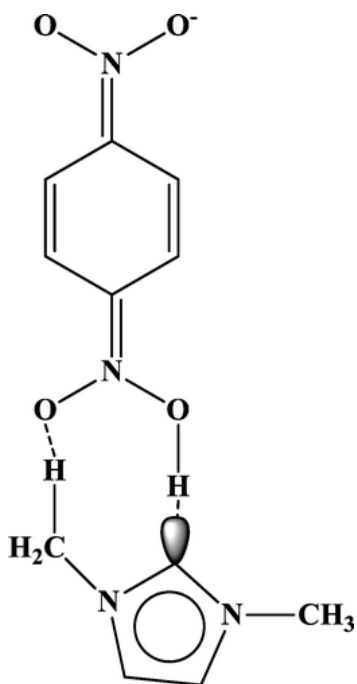
observed for 1,4-dinitrobenzene (DNB) in acetonitrile with a ΔE_{12}° value of about 200 mV. However, in BMImBF₄, a room-temperature ionic liquid (RTIL), a single wave was observed with a ΔE_{12}° value around 0 mV (based on the ΔE_p value of the cyclic voltammogram).² The shift from two one-electron waves to one two-electron wave was ascribed to ion pairing in the ionic liquid.

The sensitivity of the ΔE_{12}° on solvent and electrolyte effects has been studied by several workers. Macías-Ruvalcaba and Evans³ examined the effect of the ion pairing and activity coefficients on ΔE_{12}° of DNB in acetonitrile. An increase in ionic strength or stronger ion pairing decreased the ΔE_{12}° values. Syroeshkin et al.⁴ examined the association between 1-butyl-3-methylimidazolium ion (BMIm⁺) and the dianion of dinitrobenzene in DMF (BMIm⁺ is a common cation in RTILs). They found that up to four BMIm⁺ cations coordinated with the dianion. Even at high concentrations of BMIm⁺, though, two separate waves were observed in DMF. The FTIR spectroelectrochemistry of DNB was examined by Tian and Jin⁵ in methylene chloride. Under these conditions, both radical anion and dianion were stable. Relevant infrared bands for DNB, DNB^{•-}, and DNB²⁻ were identified.

When two waves are observed (ΔE_{12}° large and positive), it is relatively easy to determine their values from the voltammetric data. When the two waves coalesce, the determination of the ΔE_{12}° values is more problematic. A more accurate determination can be made from the concentrations of the redox species as a function of potential. For a two-electron transfer process, the concentration of the intermediate species is quite sensitive to the ΔE_{12}° value. The concentration of this species can be determined directly using spectroelectrochemistry, as long as the ΔE_{12}° is not too negative. This approach was used by Keeseey and Ryan⁶ for the determination of the ΔE_{12}° value for the sulfite reductase hemoprotein. When the ΔE_{12}° value is near zero or negative, there is no potential region where the intermediate oxidation state is the only species present. As a result, chemometric methods such as factor analysis can be used to determine the spectrum for that species, as was done with the sulfite reductase hemoprotein.⁷ This approach will be used in this work in order to more accurately determine the ΔE_{12}° value for 1,4-dinitrobenzene in a RTIL.

In a series of computational papers, Fry et al. have examined the interactions between solvent, electroactive species, and electrolyte

ions. Although the ΔE_{12}° value is quite large in the gas phase (e.g., over 4 V for anthracene), the calculated value in acetonitrile using DFT reduced to 843 mV compared well to the experimental value of 670 mV. This value was further reduced to 802 mV when ion pairing with the electrolyte was included.⁸ Further computational studies of the ion pairing between BMIm⁺ and the dianion of dinitrobenzene (DNB²⁻) in the gas phase were reported.¹ DFT calculations show that the dianion of DNB interacts with BMIm⁺ in a very unusual manner. Rather than a stacking arrangement, the BMIm⁺ ion forms an adduct where the hydrogen of the central ring carbon (C-2) has been transferred to the oxygen of the DNB²⁻ ion (Scheme 1). Previous studies have shown the DNB²⁻ has a quinoidal rather than a benzenoid structure,⁹ where the nitro groups bear most of the negative charge.



Scheme 1. Ion Pairing between DNB and BMIm⁺ As Proposed by Minami and Fry¹

The structure of mixed RTIL/organic solvents has been examined by a variety of methods recently. At low concentrations, the anions and cations of the RTIL species are solvated as most ionic compounds. As the concentration of the RTIL increases, tight ion pairs and triplet or higher aggregates are formed.¹⁰ The fact that the supramolecular structure of the pure state is maintained in mixed solvents indicates that, at least for imidazolium salt, the solution has

properties of a nanostructural material.¹⁰ These interactions are maintained even in coordinating solvents such as DMSO.^{11,12} The formation of these nanostructures in a mixed solvent can give rise to effects beyond ion pairing. If the nanostructures are large enough, RTIL/organic solvent mixtures can be viewed as having two phases on the nanoscale which may have electrochemical consequences. These issues will be pursued in this work.

There have been few studies reported on the use of spectroelectrochemistry with RTILs. Contrary to initial perceptions, RTILs that are made up of ionic species are less conductive than expected due to strong ion pairing and the high viscosity of the solvent. Using these solvents for spectroelectrochemistry in a thin-layer configuration leads to higher resistance and long electrolysis time. Most of the reports in the literature utilizing spectroelectrochemistry have involved the use of RTIL for electrodeposition¹³ or thin-film electrochemistry.¹⁴ Ogura et al.¹⁵ examined the reduction of the uranium species by the use of UV-vis spectroelectrochemistry. In this work, the advantages of using UV-vis spectroelectrochemistry to investigate the two-electron transfer process will be shown and applied to mixed RTIL/acetonitrile solutions.

Experimental Section

Chemicals

High-purity RTILs 1-butyl-3-methylimidazolium hexafluorophosphate (BMImPF₆) and 1-butyl-3-methylimidazolium bis(trifluoromethylsulfonyl)imide (BMImNTf₂) were purchased from Merck and were employed without further purification, except as noted in the text. Ethyldimethylpropylammonium bis(trifluoromethylsulfonyl)imide (EDMPAmNTf₂), 1-butyl-3-methylimidazolium chloride (BMImCl), and anhydrous acetonitrile (99.8%, water <0.001%) were purchased from Sigma-Aldrich and were used as received. Tetrabutylammonium perchlorate (TBAP, GFS Chemical Co.) was used as electrolyte in molecular solvent experiments.

Instrumentation

Cyclic voltammetry was carried out at a platinum electrode (1.6 mm) using a Model 600D Series Electrochemical Analyzer/Workstation (CHI Version 12.06). A low-volume thin-layer quartz cell which was purchased from BAS Instruments was used for UV-vis spectroelectrochemical experiments. A platinum mesh was used as working electrode, and a silver wire was used as auxiliary electrode. Potentials were measured relative to Ag/0.1 M AgNO₃/CH₃CN reference. The UV-vis spectra were recorded on a HP 8452A diode array spectrophotometer. All solutions were prepared and filled into the voltammetric or spectroelectrochemical cells in the glovebox under an argon environment. For UV-vis experiments, the entrance window of the cell was masked so that the spectral beam passed only through the working electrode.

Computational Methods

Evolving factor analysis was carried out using MATLAB, following the procedures in ref 7. The calculation of the DCVA current was also done using MATLAB and the equations in ref 6. Digisim 3.01 (BAS Instruments) was used for digital simulation in this work.

Results and Discussion

Spectroelectrochemistry in Acetonitrile

In order to compare the spectral changes of the dinitrobenzene radical anion (DNB^{•-}) and the dianion (DNB²⁻) in going from organic solvents to ionic liquids, the spectroelectrochemistry of DNB in acetonitrile was carried out. Two one-electron waves were observed, as was seen in previous work.^{2,3,16} The E° values from this work and from others are summarized in Table 1. Excellent agreement was obtained with literature values. The UV-vis spectra of the first and second reduction are shown in Figure 1. The first reduction gave rise to the DNB^{•-} (radical anion) spectrum with a band at 398 nm and another broad band starting at about 600 nm. Further reduction produced the DNB²⁻ spectrum with a band at 454 nm.

Table 1. Redox Potentials for 1,4-Dinitrobenzene in Acetonitrile and RTILs

		E_1° (V) vs Ag/AgNO ₃	E_2° (V) vs Ag/AgNO ₃	ΔE_{12}° (mV)	source
acetonitrile	cyclic voltammetry	-1.007	-1.230	223	this work
	cyclic voltammetry	-1.078 ^a	-1.278 ^a	200	ref 2
	cyclic voltammetry			221	ref 3
	cyclic voltammetry	-1.060 ^b	-1.235 ^b	175	ref 16
	DCVA	-1.004	-1.228	224	this work
	DCVA	-0.920	-0.944	24	this work
BMImpF ₆	DCVA				this work
BMIpNTf ₂	cyclic voltammetry	-0.954 ^c			this work
EDMPAmNTf ₂	cyclic voltammetry	-0.933	-0.972	39	this work

^aV vs Ag/0.1 M AgClO₄/CH₃CN.

^bV vs Fc⁺/Fc.

^cObserved E° as calculated from cyclic voltammetry for the reduction of DNB to DNB²⁻.

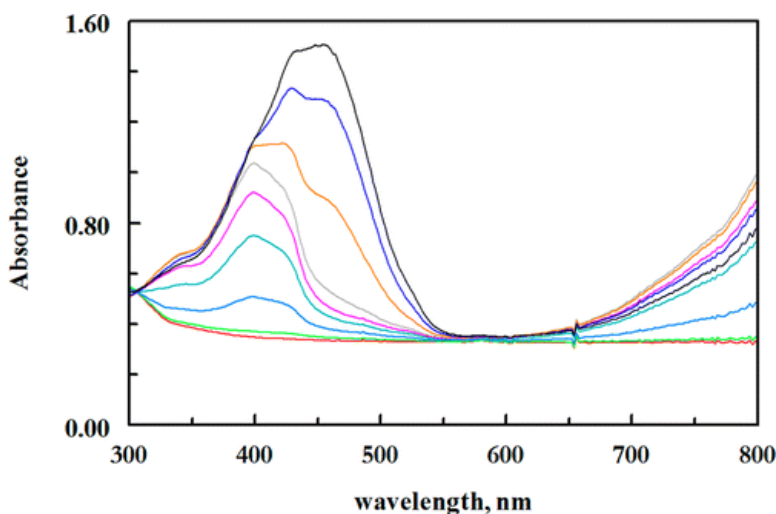


Figure 1. Spectroelectrochemistry of 0.10 mM DNB in acetonitrile. Scan rate = 2 mV/s, $E_{\text{initial}} = -0.80$ V, $E_{\text{final}} = -1.40$ V. Intermediate spectra, first reduction: -0.95, -1.01, -1.07, -1.13, -1.19. Second reduction: -1.25, -1.31 V. Supporting electrolyte: 0.10 M TBAP.

Because the waves were well-separated, there were potential regions where only the radical anion and the dianion species were the dominant species in solution. The spectrum for the dianion was obtained at -1.324 V (in the reverse scan). The absorbance due to the

radical anion had a maximum at -1.188 V (forward scan), but there was evidence of overlap between the dianion and radical anion. The spectrum for the radical anion could be more accurately obtained at -1.156 V. At this potential, there was still some starting material present, but the starting material was transparent in the visible. From an analysis of the radical anion absorbance, it was estimated that the starting material was 80% reduced at this potential. The spectra of the two species are shown in Figure 2 (dashed lines). The spectrum for $\text{DNB}^{\bullet-}$ compares well with the previously reported spectrum in DMF.¹⁷ From these spectra, the concentrations of the radical anion and dianion at each potential could be determined. Because DNB was colorless, its concentration was determined from the difference between the starting concentration (0.1 mM) and the sum of the radical anion and dianion concentrations. At the slowest scan rate used (2 mV/s), some diffusion of products from the auxiliary electrode could be observed at the end of the scan. Faster scan rates avoided such interferences.

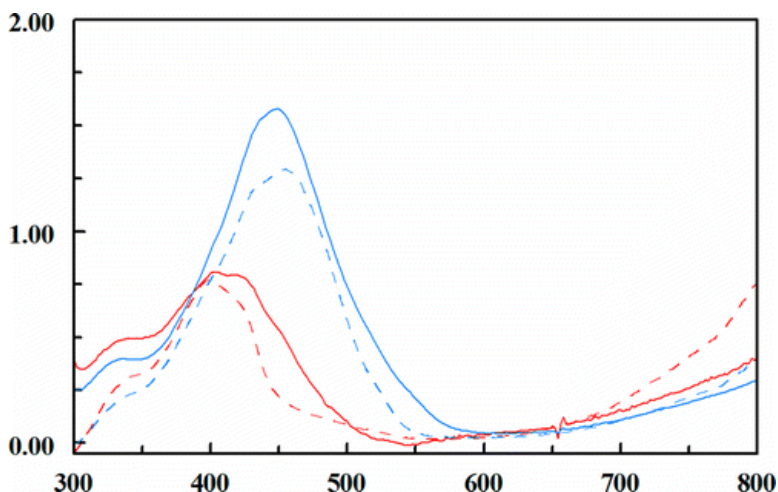


Figure 2. Calculated spectra of $\text{DNB}^{\bullet-}$ (red) and DNB^{2-} (blue) in acetonitrile (solid lines) and BImPF_6 (dashed).

The spectra obtained at 2 mV/s could be used to calculate the concentrations of the radical anion and dianion at higher scan rates. The spectrum of the interference was obtained from the final scan when the radical anion and the dianion were completely reoxidized. Because of the sloping background at short wavelengths, probably due to the cell, this background was subtracted from all spectra. From these spectra, the concentrations of the three species as a function of

potential were calculated (see Figure S1). Using these concentrations, the currents, as calculated from spectroelectrochemistry, for the first and second electron transfer were calculated using the procedure previously described.⁶ This approach is very similar to DCVA, which is morphologically equivalent to a cyclic voltammogram. Calculating the concentrations from the spectra rather than using the absorbance changes is more convenient for multielectron transfers. The results are shown in Figure 3 and Table 1. The potentials compare quite favorably with the voltammetrically obtained values. From these results, the E_1° value was found to be -1.004 V and the E_2° value was -1.228 V, giving a difference in E° values (ΔE_{12}°) of 224 mV, which compares well with the literature values determined by cyclic voltammetry (Table 1).

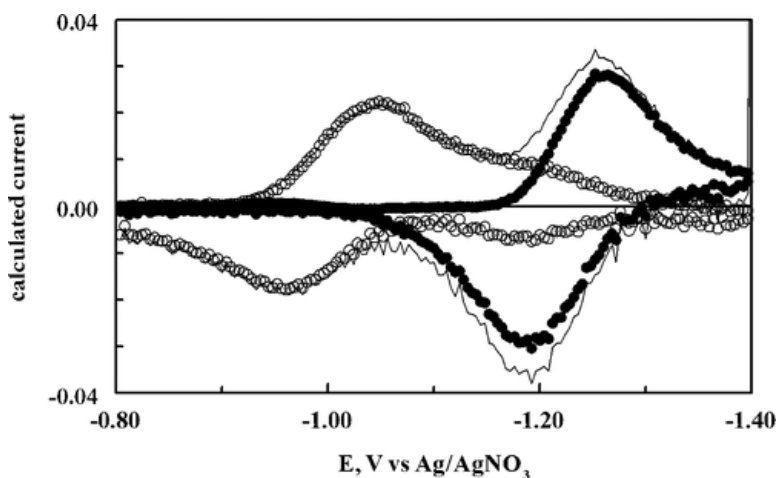


Figure 3. DCVA calculated from the concentrations of DNB, $\text{DNB}^{\cdot-}$, and DNB^{2-} from Figure S3. The open circles are due to the first reduction, closed circles are due to the second reduction alone, and the solid line is the total calculated DCVA current. Scan rate = 2.0 mV/s. Solvent: acetonitrile. Electrolyte: 0.10 M TBAP.

It should be pointed out that cyclic voltammetry yields $E_{1/2}$ values while E° values are obtained from spectroelectrochemistry. The difference between these two values is¹⁸

$$E_{1/2} = E^\circ - \frac{RT}{2nF} \ln \frac{D_{\text{O}}}{D_{\text{R}}}$$

$E_{1/2}$ values are quite close to E° values unless the diffusion coefficients differ considerably. Generally, the diffusion coefficients of the

oxidized/reduced species are similar, but O_2 in RTILs is a notable exception.¹⁹ In that case, $O_2^{\cdot-}$ was shown to have a diffusion coefficient 5 times smaller than O_2 (yielding a difference of 21 mV). This is an extreme example because the small size of O_2 allows for rapid diffusion even in RTILs. For molecules the size of DNB, the differences should be small, and where it was possible to compare our data (in mixtures), no significant differences were observed in our work.

Spectroelectrochemistry in BMImPF₆

The cyclic voltammetry and spectroelectrochemistry of DNB was carried out in BMImPF₆ (1-butyl-3-methylimidazolium hexafluorophosphate). As was observed by Fry² in BMImBF₄, only one wave was observed in the RTIL. In order to determine the difference between the two E° 's, the spectroelectrochemical data were obtained. Because of the higher viscosity of the ionic liquids as compared to acetonitrile, lower scan rates were used. For the lowest scan rate (0.1 mV/s), there was evidence of some diffusion from the auxiliary electrode at the end of the scan as was seen in acetonitrile. This effect was much less significant at higher scan rates. The spectroelectrochemical data for the forward scan rate is shown in Figure 4. The initial spectra in Figure 4 showed evidence of the radical anion around 400 nm. As the scan potential became more negative, the spectrum of the dianion dominated.

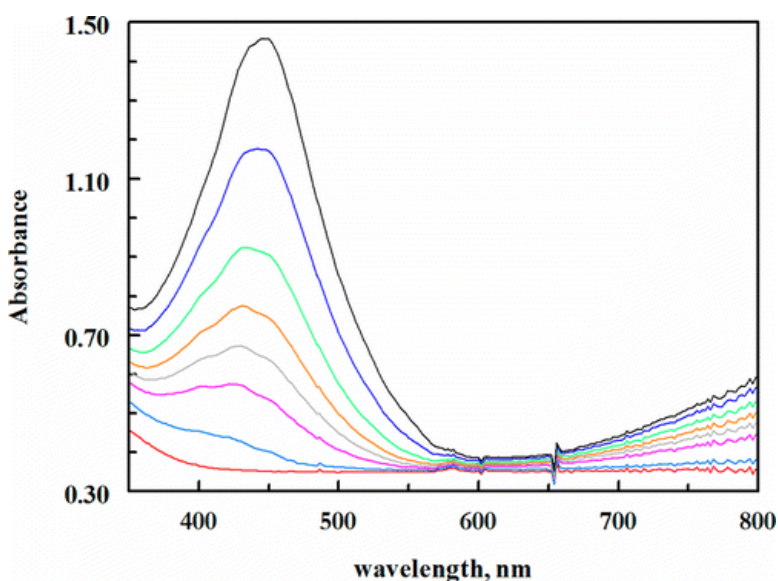


Figure 4. Spectroelectrochemistry of 0.10 mM DNB in BMImPF₆. Scan rate = 0.50 mV/s, $E_{\text{initial}} = -0.70$ V (red), $E_{\text{final}} = -1.20$ V (black). Intermediate spectra: -0.925 , -0.975 , -1.000 , -1.025 , -1.062 , and -1.125 V.

Because of the significant overlap between the spectra for the radical anion and the dianion, the approach used for acetonitrile was not practical. Evolving window factor analysis (EWFA)^{7,20} is well-suited for this type of problem. The advantage of EWFA is that the concentration of one of the species can be calculated without knowledge of the concentration of the other species.^{7,21} As a result, it was not necessary to calculate all the concentrations in order to solve this problem. As was done for acetonitrile, the background was subtracted from all spectra. Using EFA (evolving factor analysis), it was possible to determine the potentials where the radical anion and the dianion were present (see Figure S2). From this, the concentration of DNB²⁻ could be calculated as a function of potential using the procedure from ref 7 (Figure S3). As was done in acetonitrile, the spectrum of DNB²⁻ was obtained at a sufficiently negative potential where complete reduction had occurred. Using the spectrum for DNB²⁻ and the concentrations obtained from EWFA, the absorbance due to DNB²⁻ at each potential was subtracted from the experimental spectra (Figure S4). The residual spectra around -0.9 to -1.0 V looked very much like the spectrum for the radical anion in acetonitrile (Figure 2). Using the radical ion spectra obtained from this subtraction, the unnormalized concentrations of the radical were calculated using Beer's Law.

The concentrations are unnormalized because we do not know the actual molar absorptivities of the radical anion at this point, only the shape of the spectrum. Thus, while the shape of the concentration changes as a function of potential was morphologically correct, the actual concentrations were not. An examination of Figure 2 shows that the shape of the spectra for the radical anion and dianion and their λ_{max} are quite similar to the spectra in the acetonitrile. It is reasonable to expect that the ratio of ϵ 's at their respective λ_{max} values to be similar. Using this assumption, the spectrum for the radical anion was normalized. The concentrations of DNB^{•-} and DNB²⁻ could now be calculated using Beer's Law. This combination of a "soft" modeling technique such as factor analysis with a "hard" modeling technique (Beer's Law in this case) provides a powerful approach to refine the data.^{22,23} As was done for the concentrations in acetonitrile, the

concentration of the starting material was now calculated by difference. Using these concentrations, the currents due to the first and the second electron transfer (DCVA) were calculated (Figure 5). The shape of the DCVA compared well with the measured cyclic voltammogram. Although the cyclic voltammetric data are similar to the DCVA trace, the DCVA curve is somewhat broader than the voltammetric curve. Both data were obtained at the same time, but the spectral data were obtained near in the center of the electrode where ohmic resistance was higher. As the ohmic resistance affects both the forward and reverse scan, the calculated E° values (Table 1) will be minimally affected by this. The results of this work showed that the second electron transfer is still positive for the first electron transfer, but the difference is now small. The ΔE_{12}° decreased by about 170 mV (from 220 mV to 24 mV). This is very close to the value estimated by Fry² (ΔE_{12}° value of 0 mV).

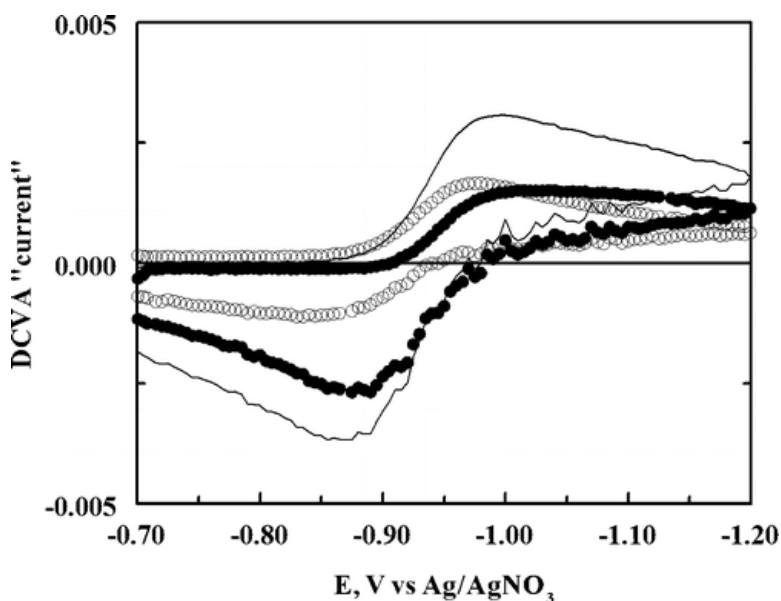


Figure 5. DCVA calculated from the concentrations of DNB, DNB^{•-}, and DNB²⁻ in BMImPF₆ calculated from the spectra in Figure 2. The open circles are due to the first reduction, closed circles are due to the second reduction alone, and the solid line is the total calculated DCVA current. Scan rate = 0.10 mV/s.

Voltammetry in Mixtures of Acetonitrile/BMImPF₆

The spectroelectrochemistry of DNB was also carried out in various ratios of mixed acetonitrile/BMImPF₆. The results are shown in Table 2. As the mole fraction of the ionic liquid increased, the difference in the E° values decreased rapidly, mostly due to the lower potential of the second electron transfer. This work parallels the previous work of Fry,² except that it was possible to measure more accurately the ΔE_{12}° values using spectroelectrochemistry when the waves merged. The solid circles in Figure 6 shows the relationship between the % BMImPF₆ and the ΔE_{12}° values. Surprisingly, a linear relationship was observed with the log % BMImPF₆.

Table 2. E° Values as a Function of % Ionic Liquid

% ionic liquid	mole fraction (RTIL)	E_1° (V) vs Ag/AgNO ₃	E_2° (V) vs Ag/AgNO ₃	$\Delta E_{12}^{\circ a}$ (mV)	method
0	0	-1.004	-1.228	224 (200)	SEC ^b
5% BMImPF ₆	0.009 66	-1.002	-1.118	116 (70)	SEC ^b
10% BMImPF ₆	0.0202	-0.982	-1.082	100 (0)	SEC ^b
20% BMImPF ₆	0.0443	-0.966	-1.048	82 (0)	SEC ^b
32% BMImPF ₆	0.107	-0.956	-1.004	48	SEC ^b
58% BMImPF ₆	0.259	-0.962	-0.994	32	SEC ^b
2% EDMPAmNTf ₂	0.0037	-0.990	-1.109	159	cyclic voltammetry
5% EDMPAmNTf ₂	0.0095	-0.977	-1.072	134	cyclic voltammetry
10% EDMPAmNTf ₂	0.020	-0.964	-1.079	115	cyclic voltammetry
1% BMImNTf ₂	0.0018	-1.026	-0.967	(192) ^c	cyclic voltammetry
2% BMImNTf ₂	0.0036	-1.038	-0.954	(167) ^c	cyclic voltammetry
5% BMImNTf ₂	0.0094	-0.991	-1.115	125 (129) ^c	cyclic voltammetry
10% BMImNTf ₂	0.020	-0.989	-1.075	86 (96) ^c	cyclic voltammetry

^aValues in parentheses are the ΔE_p values from Fry (ref 2) for BMImBF₄.

^bSpectroelectrochemistry.

^cValues in parentheses are for voltammograms where the RTIL was dried in the glovebox.

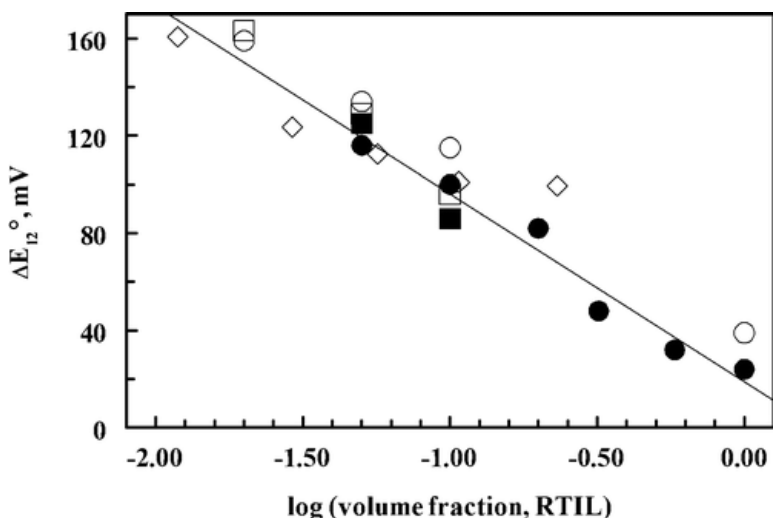


Figure 6. Variation in the ΔE_{12}° for DNB as a function of % BImPF₆ (filled circles), % EDMPAmNTf₂ (open circles), % BImNTf₂ (filled squares), dried % BImNTf₂ (open squares), and % (mol/volume) BImCl (diamonds) in acetonitrile.

This relationship can be rationalized if a mixture between a RTIL and an organic solvent is not a homogeneous solution. Previous studies have shown that strong ion pairing between the ions in the RTIL in mixed solvents.²⁴ This may indicate that RTIL/organic solvent mixtures can be better envisioned as RTIL domains and organic solvent domains, much like micellar behavior in aqueous solutions. If the solution is heterogeneous, the solutes may partition between the organic solvent domains and the RTIL domains. This can be expressed with a partition coefficient, K :

$$K_{\text{DNB}} = \frac{[\text{DNB}]_{\text{AN}}}{[\text{DNB}]_{\text{RTIL}}} = \frac{\text{no. mol}_{\text{DNB,AN}}/V_{\text{AN}}}{\text{no. mol}_{\text{DNB,RTIL}}/V_{\text{RTIL}}} \quad (1)$$

Equation 2 can be derived from K_{DNB} and the Nernst equation, as shown in the Supporting Information section.

$$E_{1/2,\text{mixed}} = E_{1/2,\text{RTIL}} - 0.059 \log \frac{V_{\text{RTIL}}}{V_{\text{AN}} + V_{\text{RTIL}}} \quad (2)$$

The slope of Figure 6 was 72 mV, reasonably close to the predicted 59 mV, given the assumptions of the derivation.

Similar results were observed by Fry for BImBF₄/acetonitrile and by Syroeshkin et al.⁴ for BImBF₄/DMF. The range of concentrations was not as large as in this work, or the ΔE_{12}° values

were difficult to calculate due to the overlap of the waves. In DMF, the decrease in the ΔE_{12}° was significantly less than that observed in acetonitrile. Acetonitrile has a much lower donor number (14.1) as compared to DMF (26.6). It has been shown that ion pair formation increases as the donor number decreases.²⁵ A stronger ion pair formation is correlated to a decrease in ΔE_{12}° . Using the observed potential shift at high concentrations of the RTIL, Syroeshkin et al. predicted that there were four cations associated with DNB^{2-} . This would be consistent with small domains of RTIL being formed within the DMF solvent, which can readily solvate DNB^{2-} .

Cyclic Voltammetry and Spectroelectrochemistry in BImNTf₂

The electrochemical study of DNB was also carried out in BImNTf₂ (NTf₂ = bis(trifluoromethylsulfonyl)imide), another commonly used RTIL. Unlike BImPF₆, two irreversible waves were observed in cyclic voltammetry with 1.0 mM DNB (Figure 7). The first wave was at -0.85 V and the second at -1.2 V. The peak current function for the first wave at 100 mV/s and 1.0 mM DNB was $9.1 \mu\text{A}/\text{mM}-(\text{V}/\text{s})^{1/2}$. This compared with a value of $5.4 \mu\text{A}/\text{mM}-(\text{V}/\text{s})^{1/2}$ in BImPF₆. Correcting for the diffusion coefficient of DNB, assuming that it is inversely proportional to the viscosity of the solvent, the ratio of the viscosity corrected current in BImNTf₂ to the current in BImPF₆ was 0.69, indicating that the first wave was between one and two electrons. At 5 mM DNB, the two waves became sharper and shifted to more positive potentials (-0.83 V and -0.94 V), but remained irreversible. At 10 mM DNB, a wave appeared with an $E_{1/2}$ of -0.954 V (Figure 7). This is consistent with the observed $E_{1/2}$ of DNB in BImPF₆ of -0.93 V. Digital simulation of the major wave (ignoring the irreversible process) is shown in Figure 7B, assuming a ΔE_{12}° value of 20 mV. The large ΔE_p could be explained by the uncompensated resistance, assuming reversible electron transfers (keeping the ΔE_{12}° value small). The increase in stability of very basic dianions in RTIL at higher substrate concentrations was also reported by Abdul-Rahim et al.,²⁶ for the voltammetry of *trans*-stilbene in another NTf₂ RTIL. The chemical irreversibility of the wave was attributed to the reaction of the stilbene dianion with trace water.

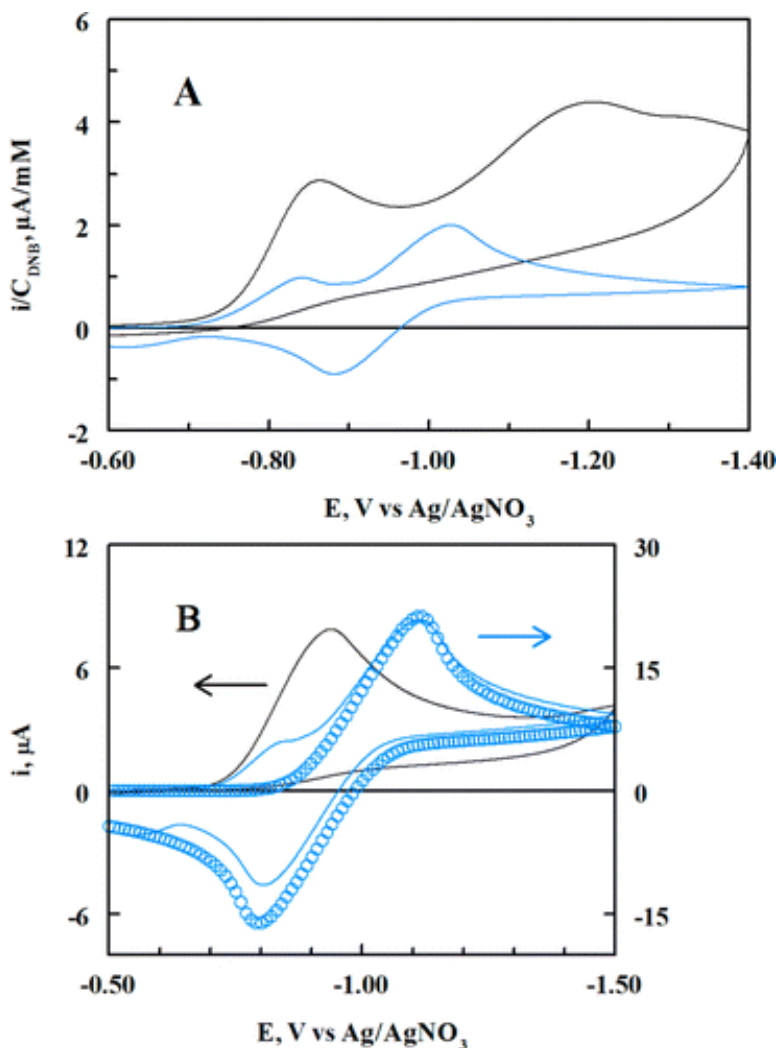


Figure 7. Cyclic voltammetry of DNB in BMImNTf₂. (A) Before water removal. (B) After water removal. Black lines: 1.0 mM DNB. Blue lines: 10 mM DNB. Scan rate = 100 mV/s. Simulated data: blue circles. For 10 mM DNB: $E_1^\circ = -0.93$ V, $E_2^\circ = -0.95$ V. Uncompensated resistance = 6000 Ω .

Spectroelectrochemistry of DNB in BMImNTf₂ gave results quite different from BMImPF₆ (see Supporting Information, Figure S5). As was observed in cyclic voltammetry, the product of the reduction was not stable, and it was not possible to reoxidize the product of either the first or the second wave back to the starting material. The spectral features of neither DNB^{•-} nor DNB²⁻ were observed in the spectra. It was not possible to carry out spectroelectrochemistry at high concentrations of DNB because the absorbance of the product formed

by the irreversible reaction was too strong to see the reversible product.

Although trace water was a reasonable source of protonation, the theoretical work of Minami and Fry¹ showed that protonation by the hydrogen attached to the C-2 carbon is also possible. To assess the importance of water, the cathodic stripping method using a gold electrode was used to monitor the water concentration.²⁷ At the levels of water that we studied, it was difficult to determine the absolute concentration, but it was possible to determine the percent reduction in water concentration. All solutions were prepared in a glovebox and studied under inert atmosphere. Water was removed by passing N₂ over the solvent heated at 70 °C. Substantial reduction in the water concentration was obtained (Figure S6), as evidenced by the complete disappearance of the water stripping peak at +0.7 V vs Ag/AgNO₃. In Figure 7, the cyclic voltammogram of DNB in the dried solvent is shown. The reduction in the water content did lead to a significant reduction in the second wave, but little change was observed in the first wave. In the driest solution, the scan rate was increased to 1000 V/s. Little change was observed in the reversibility of the wave. The concentration of DNB was then increased in the dried BImNTf₂. The voltammetric results were similar to the untreated BImNTf₂ solution, except for the disappearance of the second (water related) wave in the dried solvent. The most likely explanation for this behavior is that BIm⁺ efficiently protonates DNB²⁻, as predicted by Minami and Fry's work.²⁷ Silvester et al.²⁸ saw similar effects in the reduction of nitrobenzene in 2,3-dimethylimidazolium-NTf₂. The 2,3-dimethylimidazolium cation is less acidic than the BIm⁺ used in this work, yet protonation of the dianion was observed.

The cyclic voltammetry of DNB in mixed BImNTf₂/acetonitrile solvents was also investigated. At 1–2% BImNTf₂ in acetonitrile, there were two reversible waves (Figure 8A and Table 2). The results in Figure 8A show an excellent fit between simulated and experimental data. At 5% BImNTf₂, a new set of waves was observed at about –0.9 V on the forward scan, and an oxidation wave at –0.7 V on the reverse scan. The new wave (which was also seen in Figure 7B for high concentrations of DNB) appeared to be two overlapping waves. The new wave increased in height at 10% BImNTf₂ and overlapped with the main wave at 20% BImNTf₂. At this concentration of BImNTf₂,

the main wave became more chemically irreversible. At higher scan rates, the main wave became more chemically reversible, but the wave at -0.7 V on the reverse scan persisted. Even when the main wave was nearly reversible, poor fits were observed between simulated and experimental data for either the EE or EEC mechanisms.

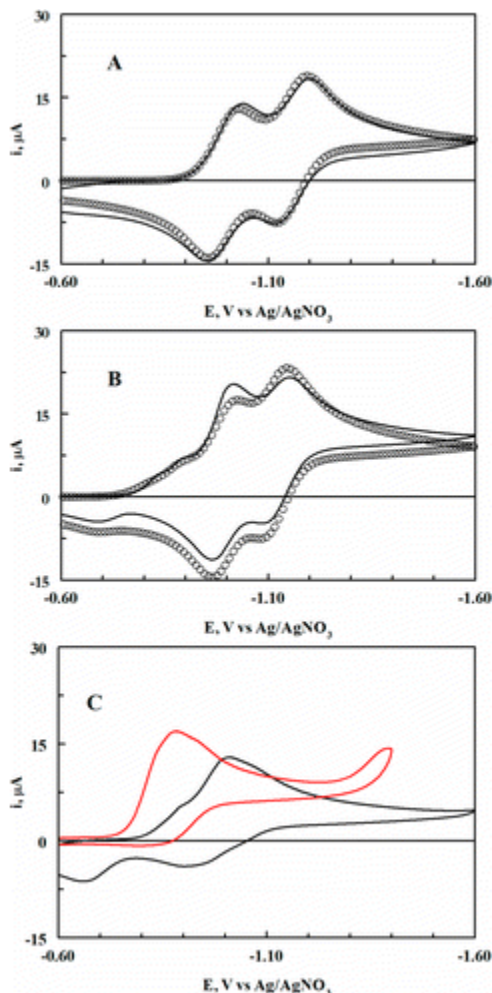
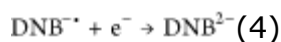
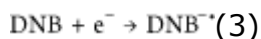


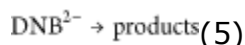
Figure 8. Cyclic voltammetry of 1.0 mM DNB in mixtures of BMImNTf₂ and acetonitrile. (A) 2% BMImNTf₂: line is the experimental data, circles are the simulated data, EE mechanism. $E_1^\circ = -0.990$ V, $E_2^\circ = -1.157$ V. Scan rate = 100 mV/s. (B) 5% BMImNTf₂: line is the experimental data, circles are the simulated data, see text for mechanism. $E_1^\circ = -0.990$ V, $E_2^\circ = -1.120$ V. Scan rate = 100 mV/s. (C) 20% BMImNTf₂ (dried): black line is the experimental data, 100 mV/s. Red line: 15% BMImNTf₂ as received. Scan rate = 200 mV/s.

The best fits for simulated/experimental data for % BMImNTf₂ \geq 5% were obtained for the following mechanism. The reduction of DNB

can occur in either the acetonitrile or RTIL nanophases. If $\text{DNB}^{\bullet-}$ and DNB^{2-} are formed in acetonitrile, the two waves are reversible:



The E° 's for these waves are given in Figure 8B for 5% BMImNTf₂. Concurrently, $\text{DNB}^{\bullet-}$ and DNB^{2-} can be formed or diffuse into the RTIL nanostructure. Once inside the RTIL nanostructure, an irreversible reaction can occur (EEC mechanism, reactions 3–5)



In Figure 8B, the best fit was observed for 14% of the reduction occurring through the EEC mechanism. If water is present in BMImNTf₂, further reduction occurs as was seen for the 100% RTIL solution (as received, not dried). A new related wave was observed at -1.4 V. For other RTILs, these two pathways cannot be directly observed because DNB^{2-} is stable in these phases, and equilibration will occur between the acetonitrile and RTIL nanophases.

The simulated mechanism above is somewhat simplistic in that it is necessary to include diffusion in/out of the nanostructures in order to provide a complete understanding of the redox process. The effect of this diffusion can be seen as the scan rate is increased (main wave more reversible). Work is in progress to modify the simulation to account for these effects and provide a fuller analysis of the overall kinetics.

The behavior that was observed is consistent with the following solution structures. For low concentrations of the RTIL, the anion and the cation are separated in acetonitrile, and ion pairing with the dianion is similar to the behavior in other molecular solvents (ion pair surrounded mostly by acetonitrile). When the nanostructural aggregates form (ion pair surrounded mostly by RTIL), the voltammetry becomes more similar to the pure RTIL, including the more energetically favorable ion pair/hydrogen bonding structure predicted by Minami and Fry.¹ Although water is involved in the further reactions of DNB^{2-} (2nd wave), the initial reaction occurs even at low concentrations of BMImNTf₂, and there is evidence that the RTIL itself is involved in the reaction of the dianion.

The explanation for the different behaviors of the RTILs studied is probably related to the structure of the RTILs. The BMImBF₄ and BMImPF₆ salts form tight ion pairs between BMIm⁺ and the small, symmetric BF₄⁻ and PF₆⁻ ions. BMImNTf₂ salts form looser ion pairs, which make this solvent more ideal for electrochemistry because of its lower viscosity and higher conductivity.²⁹ The fast reaction between DNB²⁻ and BMIm⁺ indicates that the structure predicted for this ion pair in the gas phase probably occurs in BMImNTf₂, leading to the fast protonation reaction. In BMImBF₄ and BMImPF₆, the interaction between BF₄⁻/PF₆⁻ and BMIm⁺ has a reasonably strong hydrogen bonding interaction, which is favored by the small symmetric size of the anion.²⁹ As a result, the linear structure predicted by Minami and Fry cannot occur, and a stacked ion pair is formed. This ion pair cannot easily protonate. At high concentrations of DNB, the solution will become more basic due to the protonation and reduction of the DNB²⁻ species. Under these basic conditions (due to the buildup of BMIm neutral, the product of deprotonation), the protonation reaction will be slowed down and the stable DNB²⁻ is observed.

In order to rule out the NTf₂⁻ anion as the source of the irreversible reaction, the cyclic voltammetry of DNB was carried out using EDMPAmNTf₂. The results are shown in Figure 9 and Table 1. A single reversible cyclic voltammetric wave was observed. The simulated voltammogram of DNB in EDMPAmNTf₂ is also shown in Figure 9, for a ΔE_{12}° value of 39 mV. The experimental and simulated data for 10% EDMPAmNTf₂ are also shown in Figure 9. Unlike BMImNTf₂, two reversible waves were observed with no evidence of further reaction.

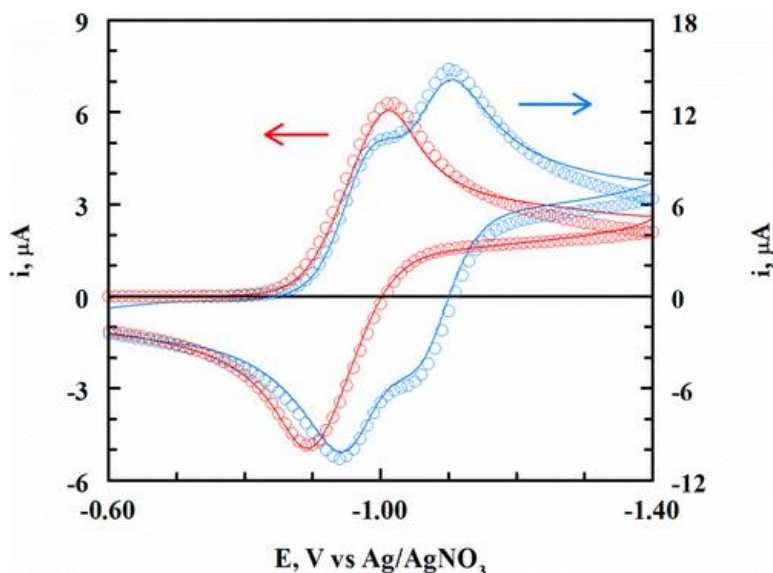


Figure 9. Cyclic voltammetry of 1.0 mM DNB in EDMPAmNTf₂ (red line) and 10% EDMPAmNTf₂/acetonitrile (blue line). Scan rate = 100 mV/s. Simulated data: red circles, $E_1^\circ = -0.933$ V, $E_2^\circ = -0.972$ V. Uncompensated resistance: 4000 Ω . Blue circles: $E_1^\circ = -0.964$ V, $E_2^\circ = -1.079$ V.

The ΔE_{12}° values for the three RTILs and one salt studied in this work are shown in Figure 6. The three RTILs yield quite similar ΔE_{12}° values over the wide range of concentrations. The ΔE_{12}° values for the alkyl cation (EDMPAmNTf₂) were slightly larger than the imidazolium salts, but the differences were probably within the uncertainties of the method. The amount of water in the RTIL had little effect, as can be seen by comparison of the dried BImNTf₂ (open squares) with the BImNTf₂ which was not dried in the glovebox (filled squares). Because of the irreversibility of the reduction at high concentrations of BImNTf₂, it was not possible to study the same range of ionic liquid concentrations with this solvent. The voltammograms for high concentrations of DNB in BImNTf₂ shows that the ΔE_{12}° value in this solvent should be similar to BImPF₆ (ΔE_{12}° much larger than 20 mV would have been detectable in the cyclic voltammetry). The final comparison is between EDMPAm⁺ and TBA⁺ (tetrabutylammonium) ion. Although EDMPAm⁺ is somewhat smaller, the difference in ion pairing between these two ions should not be great. Yet, considering that 0.10 M TBAP has a mole fraction of about 0.005 in acetonitrile, the presence of a smaller amount of EDMPAmNTf₂ (0.0037) decreases the ΔE_{12}° value by an additional 60–65 mV, more than can be explained simply by invoking ion pair formation alone.

The effect of water on the redox chemistry of DNB was not studied in detail in this work. Macías-Ruvalcaba and Evans³ have shown that high concentrations of water (around 1%) caused a significant decrease in the ΔE_{12}° values. All the work done in this report was carried out with a significantly lower concentrations of water. The presence of water at low concentrations in BMImNTf₂ had little effect on the ΔE_{12}° values of DNB (Table 2). Higher concentrations of water do lead to further reactions, probably leading to the formation of nitrosobenzenes.⁵ But the results of this work lead to the conclusion that water is either not the initial source of the protonation reaction in BMImNTf₂ or that water is much more reactive in BMImNTf₂ than in other RTILs.

The effect of ion pairing by a salt that does not form an ionic liquid (BMImCl) is also shown in Figure 6 (in this case, concentration is given in % mol/volume). The effect of higher ionic strength and ion pairing levels off at higher concentrations. At higher concentrations of salt, ion pairing between the cation and anion of the salt begins to become significant. As a result, the concentration of "free" cation (not ion paired) increases slower than the molar concentration of the salt. Similar studies were also carried out by Macías-Ruvalcaba and Evans³ for tetraalkylammonium salts. As was observed for BMImCl, the ΔE_{12}° values leveled off at higher ionic strengths, and two waves for DNB were always observed. The stronger ion pairing of BMIm⁺ was indicated by the ΔE_{12}° value leveling off at about 100 mV versus 160 mV for tetramethylammonium or 220 mV for tetrabutylammonium. Finally, even at high concentration of BMImCl, the waves remained reversible, indicating that the irreversibility of the wave in BMImNTf₂ was probably related to the nanostructure of the ionic liquid rather than the concentration of BMIm⁺ in solution.

Conclusions

The power of spectroelectrochemistry to determine the E° values for an EE mechanism, when the E° values are close together, is exemplified in this work. The merging of the first and second waves into a single wave could be followed over a range of organic solvent/RTIL mixtures. For organic solvents of low donicity such as acetonitrile, the results seem to indicate that micellar type domains may form in the mixed solvent system, yielding interesting behavior.

Comparison between RTIL/acetonitrile and RTIL/DMF (a high donicity solvent of similar dielectric constant) indicates important differences in behavior. The collapse of the two observed waves in the organic solvent occurs readily in acetonitrile mixtures, where two well - separated waves are seen in the DMF mixtures.

The identity of the anion in the imidazolium ionic liquid can have significant effects on the competition between the anionic product and the counterion. Small symmetric anions such as PF_6^- and BF_4^- form tighter ion pairs, which are favored over the anionic redox product. Larger unsymmetric anions such as NTf_2^- allow stronger hydrogen-bonding interactions between BMIm^+ and the dianionic product. The interactions are much weaker between the RTIL and monoanion. This is consistent with the work done by Nikitina et al. on the reduction of quinones in RTILs,³⁰ where the first redox potential was predicted accurately using the PCM (polarized continuum model), while the second reduction would require specific solvation at the molecular level. Further studies are being undertaken in our laboratory to provide direct experimental evidence for the two domains. The long-term implications of this observation are that it may be possible to observe RTIL behavior of anionic compounds in solutions with relatively low concentrations of RTIL. This would obviate the problem of high RTIL viscosity and the high cost of RTILs.

Supporting Information

Additional information as noted in the text. This material is available free of charge via the Internet at <http://pubs.acs.org>

The authors declare no competing financial interest.

References

- ¹Minami, Y.; Fry, A. J. AIP Conf. Proc. 2007, 963, 481– 484
- ²Fry, A. J. J. Electroanal. Chem. 2003, 546, 35– 39
- ³Macias-Ruvalcaba, N. A.; Evans, D. H. J. Phys. Chem. B 2005, 109, 14642– 14647
- ⁴Syroeshkin, M. A.; Mendkovich, A. S.; Mikhal'chenko, L. V.; Gul'tyai, V. P. Russ. Chem. Bull. 2009, 58, 1688– 1693
- ⁵Tian, D.; Jin, B. Electrochim. Acta 2011, 56, 9144– 9151
- ⁶Keesey, R. L.; Ryan, M. D. J. Electroanal. Chem. 2012, 677–680, 56– 62

- ⁷Keesey, R. L.; Ryan, M. D. *Anal. Chem.* 1999, 71, 1744– 1752
- ⁸Fry, A. J. *Electrochem. Commun.* 2005, 7, 602– 606
- ⁹Fry, A. J.; Simon, J. A.; Tashiro, M.; Yamato, T.; Mitchell, R.; Dingle, T. W.; Williams, R. V.; Mahedevan, R. *Acta Chem. Scand.* 1983, 37B, 445– 450
- ¹⁰Consorti, C. S.; Suarez, P. A. Z.; de Souza, R. F.; Burrow, R. A.; Farrar, D. H.; Lough, A. J.; Loh, W.; Da Silva, L. H. M.; Dupont, J. J. *Phys. Chem. B* 2005, 109, 4341– 4349
- ¹¹Dupont, J.; Suarez, P. A. Z.; de Souza, R. F.; Burrow, R. A.; Kintzinger, J. P. *Chem.—Eur. J.* 2000, 6, 2377– 2381
- ¹²Mele, A.; Tran, C. D.; De Paoli Lacerda, S. H. *Angew. Chem., Int. Ed.* 2003, 42, 4364– 4366
- ¹³Lahiri, A.; Olschewski, M.; Hoeffft, O.; Zein, E. A.; Endres, F. J. *Phys. Chem. C* 2013, 117, 1722– 1727
- ¹⁴Duluard, S.; Ouvrard, B.; Celik-Cochet, A.; Campet, G.; Posset, U.; Schottner, G.; Delville, M. H. *J. Phys. Chem. B* 2010, 114, 7445– 7451
- ¹⁵Ogura, T.; Takao, K.; Sasaki, K.; Arai, T.; Ikeda, Y. *Inorg. Chem.* 2011, 50, 10525– 10527
- ¹⁶Hernandez-Munoz, L. S.; Gonzalez, F. J.; Gonzalez, I.; Goulart, M. O. F.; Caxico de Abreu, F.; Ribeiro, A. S.; Ribeiro, R. T.; Longo, R. L.; Navarro, M.; Frontana, C. *Electrochim. Acta* 2010, 55, 8325– 8335
- ¹⁷Sauer, A.; Wasgestian, F.; Nickel, U. *Bull. Chem. Soc. Jpn.* 1989, 62, 2688– 2692
- ¹⁸Heyrovský, J.; Ilkovič, D. *Collect. Czech. Chem. Commun.* 1935, 7, 198– 214
- ¹⁹Buzzeo, M. C.; Klymenko, O. V.; Wadhawan, J. D.; Hardacre, C.; Seddon, K. R.; Compton, R. G. *J. Phys. Chem. A* 2003, 107, 8872– 8878
- ²⁰Ryan, M. D.; Keesey, R. L. *AIP Conf. Proc.* 2007, 963, 491– 494
- ²¹Malinowski, E. R. *J. Chemom.* 1992, 6, 29– 40
- ²²Atifi, A.; Czarnecki, K.; Mountacer, H.; Ryan, M. D. *Environ. Sci. Technol.* 2013, 47, 8650– 8657
- ²³Fernandez, C.; de Juan, A.; Callao, M. P.; Larrechi, M. S. *Chemom. Intell. Lab. Syst.* 2012, 114, 64– 71
- ²⁴Kalugin, O. N.; Voroshylova, I. V.; Riabchunova, A. V.; Lukinova, E. V.; Chaban, V. V. *Electrochim. Acta* 2013, 105, 188– 199
- ²⁵Gutmann, V. *Chem. Ber.* 1971, 7, 102– 107
- ²⁶Abdul-Rahim, O.; Simonov, A. N.; Rüther, T.; Boas, J. F.; Torriero, A. A. J.; Collins, D. J.; Perlmutter, P.; Bond, A. M. *Anal. Chem.* 2013, 85, 6113– 6120
- ²⁷Zhao, C.; Bond, A. M.; Lu, X. *Anal. Chem.* 2012, 84, 2784– 2791
- ²⁸Silvester, D. S.; Wain, A. J.; Aldous, L.; Hardacre, C.; Compton, R. G. *J. Electroanal. Chem.* 2006, 596, 131– 140
- ²⁹Hapiot, P.; Lagrost, C. *Chem. Rev.* 2008, 108, 2238– 2264

³⁰Nikitina, V. A.; Nazmutdinov, R. R.; Tsirlina, G. A. J. Phys. Chem. B 2011, 115, 668– 677